

August 1972

Raman Scattering from ZnS Polytypes

J. Schneider

University of Nebraska-Lincoln

Roger D. Kirby

University of Nebraska-Lincoln, rkirby1@unl.edu

Follow this and additional works at: http://digitalcommons.unl.edu/physics_kirby



Part of the [Physics Commons](#)

Schneider, J. and Kirby, Roger D., "Raman Scattering from ZnS Polytypes" (1972). *Roger Kirby Publications*. 30.
http://digitalcommons.unl.edu/physics_kirby/30

This Article is brought to you for free and open access by the Research Papers in Physics and Astronomy at DigitalCommons@University of Nebraska - Lincoln. It has been accepted for inclusion in Roger Kirby Publications by an authorized administrator of DigitalCommons@University of Nebraska - Lincoln.

M. Blackman, *ibid.* **86**, 421 (1933); see also J. Neuberger and R. D. Hatcher, *J. Chem. Phys.* **34**, 1733 (1961).

³³B. Szigeti, *Proc. Roy. Soc. (London)* **A252**, 217 (1959); **A258**, 377 (1960); in Ref. 26, p. 377.

³⁴D. Kleinman, *Phys. Rev.* **118**, 118 (1960).

³⁵V. V. Mitskevitch, *Fiz. Tverd. Tela* **3**, 3036 (1961); **4**, 3035 (1962) [*Sov. Phys. Solid State* **3**, 2211 (1962); **4**, 2224 (1963)].

³⁶C. Flytzanis (unpublished); see also, C. Flytzanis, in *Treatise in Quantum Electronics*, edited by H. Rabin and C. L. Tang (Wiley, New York, to be published), Vol. I.

³⁷A. Dalgarno and J. Lewis, *Proc. Roy. Soc. (London)* **A233**, 701 (1956); C. Schwartz, *Ann. Phys. (N. Y.)* **6**, 156 (1959); see also M. Karplus and J. Kolker, *J. Chem. Phys.* **39**, 2011 (1963).

³⁸For a calculation of the Raman tensor of diatomic molecules with this model see T. Veach Long and R. A. Plane, *J. Chem. Phys.* **43**, 457 (1965); for a more detailed discussion of different calculations of $\alpha^{(1)}$ for molecules see also J. Tang and A. C. Albrecht, *ibid.* **49**, 1144 (1968).

³⁹C. L. Tang and C. Flytzanis, *Phys. Rev. B* **4**, 2520 (1971).

⁴⁰S. Ushioda, A. Pinczuk, W. Taylor, and E. Burstein, in *II-VI Semiconducting Compounds*, edited by D. G. Thomas (Benjamin, New York, 1968).

⁴¹A. Moradian and A. L. McWhorter, in *Proceedings of the International Conference on Light Scattering in Solids, New York University*, edited by G. B. Wright (Springer-Verlag, New York, 1968).

⁴²I. P. Kaminow and W. D. Johnston, *Phys. Rev.* **188**, 1209 (1969).

⁴³G. D. Boyd, T. J. Bridges, M. A. Pollack, and E. H. Turner, *Phys. Rev. Letters* **26**, 387 (1971). The separation out of $\chi_M^{(2)}$ of the contribution $\chi_H^{(2)}$, $\chi_N^{(2)}$ given there is not altogether correct since a contribution $2C_1\chi_E^{(2)}$ is included which is of an entirely different nature [compare (3.39) with (3.46b)].

⁴⁴R. Geick, *Phys. Rev.* **138**, A1495 (1965).

⁴⁵J. J. Wynne and N. Bloembergen, *Phys. Rev.* **188**, 1211 (1969).

⁴⁶In Ref. 7, using an old value for $e_S^* = [3/(\epsilon_\infty + 2)]e_T^* = 1.2$, it was found that $C_1 \approx 0.2$ for CuCl. This value for e_S^* , however is incorrect; e_T^* has been remeasured recently by Iwasa [thesis (University of Pennsylvania) (unpublished)] and found $e_T^* = 1.2$ which gives $e_S^* = 0.5$ ($\epsilon_\infty = 3.5$ and $\epsilon_0 = 6.5$). With e_S^* smaller than unity repeating the argument of Ref. 7 one obtains $C_1 \approx -1.2$; for this crystal e_T^* is positive or equivalently Cu behaves as a positive ion. A simple calculation predicts, then, that the signs of C_i alternate. Further, due to the d states it is predicted (Refs. 3 and 39) that $\chi_E^{(2)}$ is negative for this compound. The simple calculation, then, predicts that $\chi_M^{(2)} > 0$ with the axis conventions of Fig. 1 and almost by an order of magnitude larger than $-\chi_E^{(2)}$.

⁴⁷R. L. Kelly, *Phys. Rev.* **151**, 721 (1966).

⁴⁸L. R. Swanson and Maradudin, *Solid State Commun.* **8**, 589 (1970).

⁴⁹We point out that in the case of purely ionic cubic crystals like NaCl, where the effective field factor $f = (\epsilon_\infty + 2)/3$ can be used, the expressions for e_T^* , ω_T , $\mu^{(2)}$, and $\phi^{(3)}$ derived in the present work reduce to the ones given by Szigeti, Refs. 13, 24, and 34, respectively. However, this author does not take into account the contributions in $\mu^{(2)}$ and $\phi^{(3)}$ originating from β_E and $\alpha^{(1)}$ and which provide additional phonon interaction terms (see Ref. 36).

⁵⁰We restrict ourselves to the coefficient $\chi_{zzz}^{(2)}$ in these compounds; the z axis in wurzite structure is equivalent to one of the [111] directions in the zinc-blende structure and the axis convention of Fig. 1 is still valid.

⁵¹This statement is correct only if $e^* < 0$ with the axis conventions adopted. This seems to be confirmed by the sign of the experimental values of $\chi_{EO}^{(2)} - \chi_E^{(2)}$.

⁵²Slightly different classification is used in Ref. 3.

⁵³P. D. Maker and R. W. Terhune, *Phys. Rev.* **137**, A801 (1965).

⁵⁴E. Yablonovitch, C. Flytzanis, and N. Bloembergen, in *Seventh International Quantum Electronics Conference, Montreal, Canada, 1972* (unpublished); and (unpublished).

Raman Scattering from ZnS Polytypes*

J. Schneider[†] and R. D. Kirby[‡]

Department of Physics and Materials Research Laboratory, University of Illinois, Urbana, Illinois 61801

(Received 17 February 1972)

The Raman spectra of the 2H and 4H structures of ZnS have been measured between room temperature and 60 K, and compared with the spectra from zinc blende ZnS. The observed phonons in each case are in good agreement with those expected from the known structural differences.

ZnS is known¹ to crystallize in many different crystal structures belonging to the cubic, hexagonal, and rhombohedral space groups. All such ZnS polytypes¹ can be constructed from alternating zinc and sulphur planes which are perpendicular to

the cubic [111] or hexagonal [0001] axis, with the various polytypes being distinguished only by the stacking sequence of the planes. The most important characteristic which distinguishes one polytype from another is then the length c of the funda-

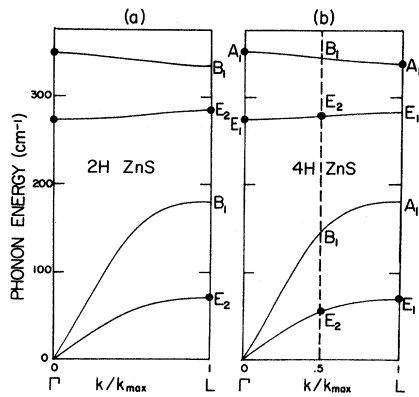


FIG. 1. Schematic drawing of the axial-direction dispersion curves for zinc-blende ZnS. (a) Phonon-dispersion curves based on the $2H$ Raman data. (b) Phonon-dispersion curves based on the $4H$ Raman data. In both (a) and (b), the closed circles are the observed frequencies at room temperature.

mental translation along the axis perpendicular to the atomic planes. The lengths c for the various polytypes are, to a very good approximation, integer multiples of the cubic-zinc-blende value of c . For such a situation, it has been pointed out² that increasing c in multiples of the cubic value corresponds to a folding over of the cubic Brillouin zone along $[111]$, so that zone-boundary and

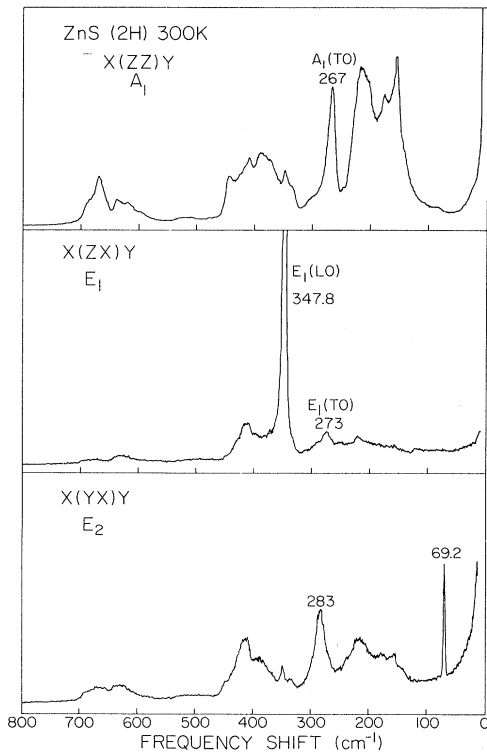


FIG. 2. Raman spectra of $2H$ ZnS at room temperature.

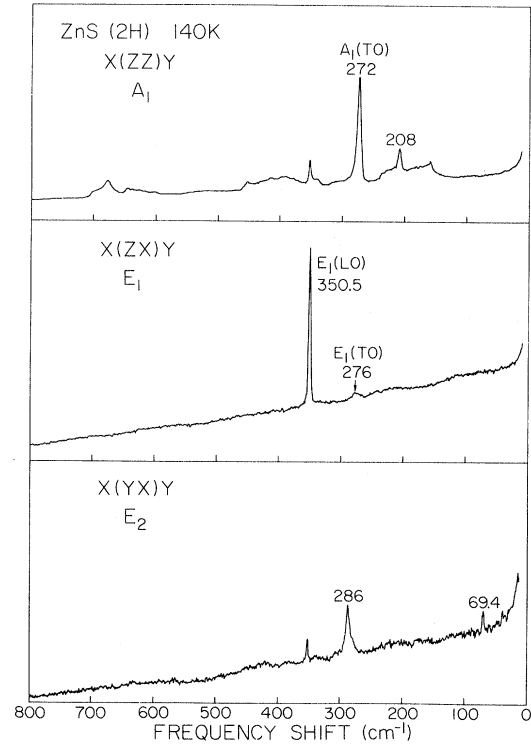


FIG. 3. Raman spectra of $2H$ ZnS at 140 K.

perhaps intermediate- k -value zinc-blende phonons are transformed into zone-center phonons for the higher polytypes. Some of these new zone-center phonons are then accessible to Raman and infrared measurements. This technique has been fully exploited to obtain rather accurate dispersion curves along $[111]$ in SiC.³

There have been a number of Raman studies of ZnS since the investigation of Poulet, Klee, and Mathieu.⁴ Nilsen⁵ has measured the one- and two-phonon Raman spectra of cubic ZnS. Brafman and Mitra⁶ and Vetelino *et al.*⁷ have made room-temperature Raman measurements on the $2H$, $4H$, and $6H$ modifications of ZnS. The work to be presented here on the $2H$ and $4H$ polytypes should be considered an extension of these earlier investigations in that we have observed more of the possible Raman-active phonons, have measured the A_1 - E_1 TO splittings, and have made some temperature-dependence measurements.

The Raman measurements were made using an argon-krypton mixed-gas laser and a Spex double monochromator. The results to be shown were obtained using the 4880-\AA argon laser line with about 400 mW of power. Measurements at other laser excitation frequencies were made to distinguish fluorescence lines from the spectra. The output of a neon lamp was focused on the sample and imaged on the monochromator entrance slit

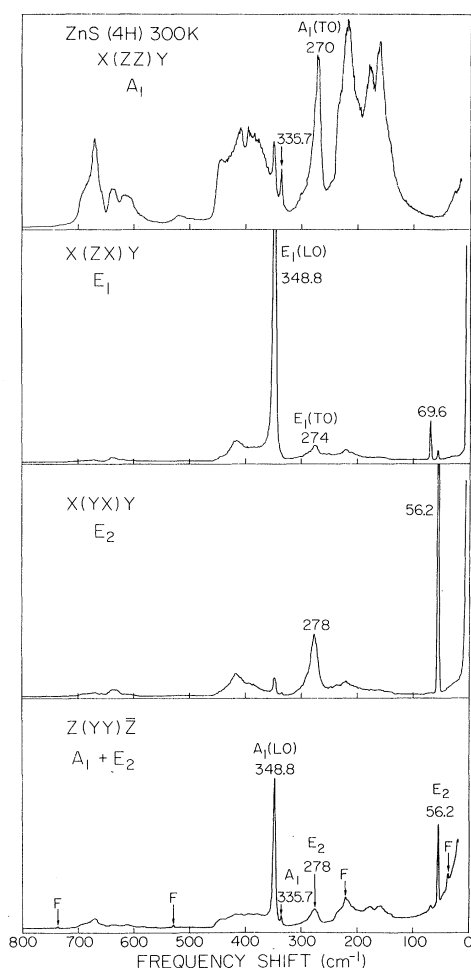


FIG. 4. Raman spectra of 4H ZnS at room temperature. Nonlasing fluorescence lines are denoted by "F."

along with the Raman-scattered light in order to introduce calibration lines into the observed spectra. The instrumental resolution was 3 cm^{-1} .

The 2H and 4H ZnS polytypes used in this investigation were vapor-grown platelets of thickness $50\text{--}150 \mu$. After selection for uniform birefringence their structures were determined from Laue back-reflection photographs. The samples for which spectra are to be shown were found to be pure polytypes, whereas most other samples were heavily stack faulted and likely consisted of many different polytypes separated by lines of high birefringence. The Raman spectra of such samples often showed additional lines, particularly in the E_2 spectra at low frequencies. Other samples studied include naturally occurring crystals of the zinc-blende structure and melt-grown crystals. Laue photographs of the melt-grown crystals showed them to be primarily of the "twinned cubic" variety,^{8,9} consisting of microcrystalline cubic regions rotated 180° about a common [111] axis.

This serves to make a particular [111] axis unique, so that the crystal appears to be uniaxial when investigated under crossed polaroids. Laue photographs taken along the unique [111] axis had a definite "hexagonal" symmetry, indicating that the two possible orientations of the microcrystals occurred in about equal numbers. It is worth mentioning that the Raman spectra of our melt-grown twinned cubic crystals, when measured in a "hexagonal" scattering geometry, appear to be identical with the spectra obtained from melt-grown samples by Arguello *et al.*¹⁰ and attributed by them to wurzite (2H)ZnS.

Zinc-blende ZnS has two optic phonons, both of which are Raman active. Nilsen⁵ has measured the LO and TO frequencies at room temperature to be 352 and 271 cm^{-1} , respectively. The wurzite 2H structure has a c value twice as large as the zinc-blende structure, so that zinc-blende zone-boundary phonons at the point L of the Brillouin zone will be transformed into 2H zone-center

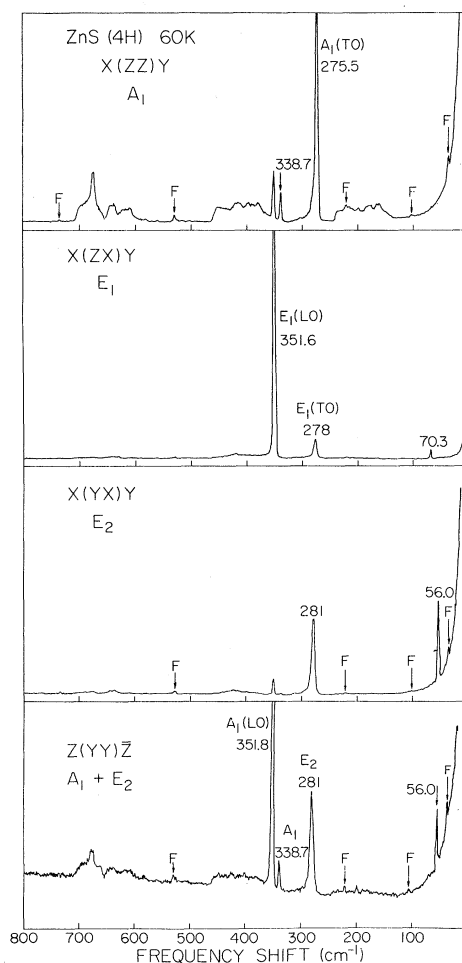


FIG. 5. Raman spectra of 4H ZnS at 60 K. Nonlasing fluorescence lines are denoted by "F."

TABLE I. Phonon frequencies in 2H ZnS.

Phonon	Frequency at 300 K (cm ⁻¹)	Frequency at 140 K (cm ⁻¹)
A ₁ (LO)	(n. o.) ^a	(n. o.)
E ₁ (LO)	347.8	350.5
A ₁ (TO)	267	272
E ₁ (TO)	273	276
TO(L)-E ₂	283	286
TA(L)-E ₂	69.2	69.4

^a(n. o.) is not observed.

phonons. This is illustrated in Fig. 1(a), which shows a schematic drawing of the zinc-blende dispersion curves along Γ -L. The 2H optic phonons corresponding to LA(L) and LO(L) both have B₁ symmetry and hence are Raman inactive. The phonons arising from TA(L) and TO(L) have E₂ symmetry and are Raman active. In addition, the hexagonal symmetry of the 2H crystal results in A₁-E₁ splittings of the TO and LO phonons.

Figures 2 and 3 show the Raman spectra of the 2H ZnS polytype for temperatures of 300 and 140 K, respectively. Our scattering notation, as in for example $[x(zx)y]$, is that of Damen, Porto, and Tell,¹¹ where z is parallel to the crystal c axis. For the scattering geometries shown here, the created phonon propagates perpendicular to the c axis. No back-scattering measurements along the c axis could be made because of the absence of a crystal surface perpendicular to the c axis. Even the 90° scattering data were difficult to obtain because the surface which the laser light entered was wedge shaped. In spite of this, there appeared to be little depolarization of the incident beam since the observed phonons have well-defined symmetries. All of the Raman-active phonons expected for the wurtzite 2H structure have been observed except for the A₁ LO phonon which can only be seen in back or forward scattering. The data points in Fig. 1(a) are our measured room-temperature 2H phonon frequencies. In addition, a weak A₁ symmetry line appears at 208 cm⁻¹ in the 140-K spectrum. It is also present in spectra taken at 25 K and thus appears to be first order. We do not yet have an explanation for this line.

The 4H ZnS polytype has a c value four times that of zinc blende, or twice the 2H value, which leads to a second folding of the cubic Brillouin zone. In addition to the zone-boundary phonons at point L, the phonons at $k/k_{\max}=0.5$ are also transformed into zone-center phonons, as indicated in Fig. 1(b). For 4H, the points LA(L) and LO(L) have A₁ symmetry and the points TA(L) and TO(L) have E₁ symmetry. All of these phonons should be Raman active. From $k/k_{\max}=0.5$, there should be

two inactive B₁ phonons and two active E₂ phonons. Each of these phonons is in principle doubled because of the energy discontinuity at $k/k_{\max}=0.5$.¹²

Figures 4 and 5 show the Raman spectra of the 4H ZnS polytype for temperatures of 300 and 60 K, respectively. As expected, these spectra are more complicated than the 2H spectra, and additional phonons are observed; an A₁ near 338 cm⁻¹ and an E₂ near 281 cm⁻¹ and another near 56 cm⁻¹. The 70-cm⁻¹ E₂ phonon in the 2H spectra has become E₁ symmetry, in agreement with theory. No evidence of doubling of the E₂ phonons was found, so that these components are either unresolved or too weak to be observed. Also not observed were the phonons arising from LA(L) (A₁ symmetry—expected near 195 cm⁻¹)¹³ and TO(L) (E₁ symmetry—expected near 290 cm⁻¹). Again, the data points in Fig. 1(b) are our measured room-temperature frequencies.

We should make one other comment here. The results of the back-scattering experiments are not accurate with regard to the relative intensities of the A₁ and E₂ phonons. The depolarized spectrum $z(xy)\bar{z}$, which should yield only E₂ phonons, was found to be nearly identical to the $z(yy)\bar{z}$ spectra shown in the figures. This effect is probably caused by depolarization of both the incident (converging) and scattered (diverging) beams due to the birefringence of the ZnS sample for light propagating nearly parallel to the optic axis. This depolarization mechanism has been described in some detail by Porto, Giordmaine, and Damen.¹⁴

Our measured phonon frequencies are summarized in Table I for 2H ZnS and in Table II for the 4H polytype. It is felt that the listed frequencies are accurate to ± 1 cm⁻¹ for the broad lines and to ± 0.5 cm⁻¹ for the narrow lines. There are some disagreements with the previously published results on 2H ZnS. In particular, with the exception of the E₁(T) phonon, our measured frequencies are all 3–6 cm⁻¹ less than those of Brafman and

TABLE II. Phonon frequencies in 4H ZnS.

Phonon	Frequency at 300 K (cm ⁻¹)	Frequency at 140 K (cm ⁻¹)	Frequency at 60 K (cm ⁻¹)
A ₁ (LO)	348.8	351.7	351.8
E ₁ (LO)	348.8	351.6	351.6
A ₁ (TO)	270	274.5	275.5
E ₁ (TO)	274	277.5	278
LO(L)-A ₁	335.7	338.0	338.7
TO(L)-E ₁	(n. o.) ^a	(n. o.)	(n. o.)
LA(L)-A ₁	(n. o.)	(n. o.)	(n. o.)
TA(L)-E ₁	69.6	69.8	70.3
TO($k/k_{\max}=0.5$)-E ₂	278	281	281
TA($k/k_{\max}=0.5$)-E ₂	56.2	56.3	56.0

^a(n. o.) is not observed.

Mitra.⁶ The largest discrepancy, and the only one outside the combined experimental uncertainty of the two sets of measurements, is for the $A_1(\text{TO})$ phonon. We found the $A_1(\text{TO})$ phonon to be at $(267 \pm 1) \text{ cm}^{-1}$, whereas Brafman and Mitra found the value to be $(273 \pm 3) \text{ cm}^{-1}$. These apparent frequency shifts could be due to the presence of unwanted impurities in our nominally pure samples, and this could also explain the as yet unidentified

208- cm^{-1} line.

We wish to thank Dr. Deiter Langer and Dr. Y. S. Park of Aerospace Research Laboratories, Wright Patterson Air Force Base, Ohio for helpful discussions as well as for providing the ZnS vapor-grown platelet crystals for this work. The advice and efforts of Dr. Miles V. Klein, in whose laboratory this work was performed is gratefully acknowledged.

*This work was supported in part by the Advanced Research Projects Agency under Contract No. HC 15-67-C-0221.

†Present address: Department of Physics, University of Dayton, Dayton, Ohio 45409.

‡Present address: Behlen Laboratory of Physics, University of Nebraska, Lincoln, Neb. 68508.

¹A. R. Verma and P. Krishna, *Polymorphism and Polytypism in Crystals* (Wiley, New York, 1966).

²Lyle Patrick, *Phys. Rev.* **167**, 809 (1968).

³D. W. Feldman, James H. Parker, Jr., W. J. Choyke, and Lyle Patrick, *Phys. Rev.* **173**, 787 (1968), and references therein.

⁴H. Poulet, W. E. Klee, and J. P. Mathieu, in *Proceedings of the International Conference on Lattice Dynamics, Copenhagen, 1963* (Pergamon, New York, 1965), pp. 337-341.

⁵W. G. Nilsen, *Phys. Rev.* **182**, 838 (1969).

⁶O. Brafman and S. S. Mitra, *Phys. Rev.* **171**, 931 (1968).

⁷J. F. Vetelino, S. S. Mitra, O. Brafman, and T. C. Damen, *Solid State Commun.* **7**, 1809 (1969).

⁸Atsuko Ebina and Tadashi Takahashi, *J. Appl. Phys.* **38**, 3079 (1967).

⁹G. V. Anan'eva, K. K. Dubenskii, A. I. Ryskin, and G. I. Khil'ko, *Fiz. Tverd. Tela* **10**, 1800 (1968) [*Sov. Phys. Solid State* **10**, 1417 (1968)].

¹⁰C. A. Arguello, D. L. Rousseau, and S. P. S. Porto, *Phys. Rev.* **181**, 1351 (1969).

¹¹T. C. Damen, S. P. S. Porto, and B. Tell, *Phys. Rev.* **142**, 570 (1966).

¹²H. Jones, *The Theory of Brillouin Zones and Electronic States in Crystals* (North Holland, Amsterdam, 1960), Chap. 5.

¹³L. A. Feldkamp, G. Venkataraman, and J. S. King, *Solid State Commun.* **7**, 1571 (1969); L. A. Feldkamp, D. K. Steinman, N. Vagelatos, J. S. King, and G. Venkataraman, *J. Phys. Chem. Solids* **32**, 1572 (1971).

¹⁴S. P. S. Porto, J. A. Giordmaine, and T. C. Damen, *Phys. Rev.* **147**, 608 (1966).

Optical Spectra of Some II-IV-V₂ Ternary Compounds

S. E. Stokowski*

Bell Telephone Laboratories, Murray Hill, New Jersey 07974

(Received 28 December 1972)

The polarized-reflectance spectra between 2.0 and 5.2 eV and the logarithmic derivative of the reflectance at 2 K for the ternary compounds ZnSiAs₂, CdSiAs₂, CdSnAs₂, and CdSnP₂ are reported. All the structure observed in previous electroreflectance data is seen in the logarithmic-derivative spectra plus some additional weak structure. The E_1 reflectance structures consist of three or more peaks; it is suggested that the additional splitting of the E_1 transitions is due to a separation in energy of the Λ and L critical points. No evidence is found in the optical spectra for the presence of Γ_{15}^v to X_1^c or X_3^c "pseudo-direct" transitions. The chalcopyrite crystalline structure, how it relates to zinc blende, its effect on the band structure, and group theory as applied to the chalcopyrites are discussed in detail.

I. INTRODUCTION

Interest in the I-III-VI₂ and II-IV-V₂ ternary compounds which crystallize in the chalcopyrite structure has been stimulated by their possible use as nonlinear optical materials^{1,2} and as visible-emitting diodes. From a fundamental point of view a study of these compounds is a logical step in extending present knowledge about the properties of $A^N B^{8-N}$ binary materials to the next-higher level of

complexity; in these ternary compounds one is dealing with two different bonds rather than the single bond of the binaries. The optical spectra of the chalcopyrites is one very important property which can provide information about the band structure and thus, the bonding of these compounds. In particular, the experimentally obtained logarithmic derivative of the reflectance can provide a direct test for any band calculation. In this paper the optical spectra (reflectance and logarithmic